PAPER • OPEN ACCESS

Decoherence effects in non-classicality tests of gravity

View the article online for updates and enhancements.

New Journal of Physics

The open access journal at the forefront of physics

PAPER

Decoherence effects in non-classicality tests of gravity

Simone Rijavec[1,*] , **Matteo Carlesso**[2,3] , **Angelo Bassi**[2,3] , **Vlatko Vedral**[1,4,5] and **Chiara Marletto**[1,4,5]

1. Clarendon Laboratory, University of Oxford, Parks Road, Oxford OX1 3PU, United Kingdom
2. Department of Physics, University of Trieste, Strada Costiera 11, 34151 Trieste, Italy
3. Istituto Nazionale di Fisica Nucleare, Trieste Section, Via Valerio 2, 34127 Trieste, Italy
4. Centre for Quantum Technologies, National University of Singapore, 3 Science Drive 2, 117543, Singapore
5. Department of Physics, National University of Singapore, 2 Science Drive 3, 117542, Singapore
* Author to whom any correspondence should be addressed.

E-mail: simone.rijavec@physics.ox.ac.uk

Abstract

The experimental observation of a clear quantum signature of gravity is believed to be out of the grasp of current technology. However, several recent promising proposals to test the possible existence of non-classical features of gravity seem to be accessible by the state-of-art table-top experiments. Among them, some aim at measuring the gravitationally induced entanglement between two masses which would be a distinct non-classical signature of gravity. We explicitly study, in two of these proposals, the effects of decoherence on the system's dynamics by monitoring the corresponding degree of entanglement. We identify the required experimental conditions necessary to perform successfully the experiments. In parallel, we account also for the possible effects of the continuous spontaneous localization (CSL) model, which is the most known among the models of spontaneous wavefunction collapse. We find that any value of the parameters of the CSL model would completely hinder the generation of gravitationally induced entanglement.

1. Introduction

Testing the quantumness of gravity represents an outstanding challenge that has been approached from different perspectives [1]. Clearly the direct detection of the graviton—the quantum mediator of the gravitational interaction—would undeniably confirm the quantumness of gravity. However, the current state-of-art technology is not yet sufficiently advanced to allow for such a detection [2, 3], and alternative paths need to be explored. Several low-energy table-top experiments were proposed over the years, which aim at testing effects resulting from either of a quantum [4–8] or a classical theory of gravity [9]. Among such proposals, we focus on two of them, one by Bose *et al* [10] and Marletto–Vedral [11] (BM) and one by Krisnanda *et al* [12], which seem to be within reach of the current technology. They rely on the generation of a gravitationally induced entanglement between two masses, which would work as a witness of the non-classical nature of the gravitational mediator [10, 11]. This new approach to witnessing non-classical features of gravity has been subject of intense study and debate [13–26], and is at the core of several recent experimental proposals [27–31]. Since the gravitational interaction is weak, one needs to employ large masses to achieve a measurable amount of entanglement in an experimentally reasonable time. However, larger masses are strongly affected by the environmental noises. Such effects, in particular decoherence, suppress quantum superpositions and thus hinder the entanglement generated by gravity. Therefore, it is crucial to consider explicitly environmental decoherence effects in the dynamics of the system. Moreover, since these setups are very sensitive to any source of decoherence, one should account also for non-standard decoherence sources as those described by models of spontaneous wavefunction collapse. These models represent possible solutions to the quantum measurement problem. They modify the standard evolution due to quantum mechanics by introducing stochastic and non-linear terms in the Schrödinger equation
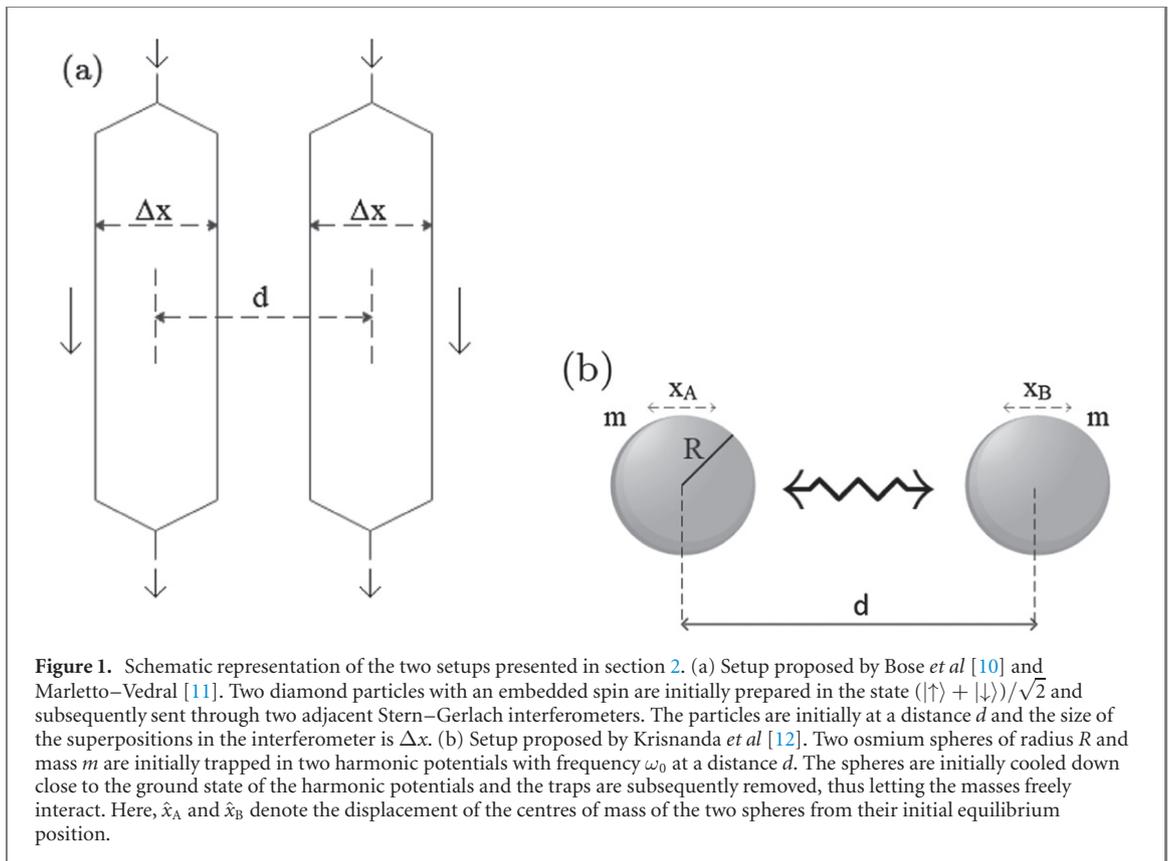
Figure 1. Schematic representation of the two setups presented in section 2. (a) Setup proposed by Bose *et al* [10] and Marletto–Vedral [11]. Two diamond particles with an embedded spin are initially prepared in the state $(|\uparrow\rangle + |\downarrow\rangle)/\sqrt{2}$ and subsequently sent through two adjacent Stern–Gerlach interferometers. The particles are initially at a distance d and the size of the superpositions in the interferometer is Δx. (b) Setup proposed by Krisnanda *et al* [12]. Two osmium spheres of radius R and mass m are initially trapped in two harmonic potentials with frequency ω_0 at a distance d. The spheres are initially cooled down close to the ground state of the harmonic potentials and the traps are subsequently removed, thus letting the masses freely interact. Here, $\hat{x}_A$ and $\hat{x}_B$ denote the displacement of the centres of mass of the two spheres from their initial equilibrium position.

[32, 33]. While these models are still under active testing [34–37], it is instructive to account for their possible effects in these setups. Additional decoherence effects can rise from different processes related to gravity, as those proposed and analysed in [38–50]. Our approach can easily be modified to include them, and the analysis is left for future research.

In this work, by building on the first analysis performed in [51, 52] for the setup of Bose *et al*, we study the decoherence effects on the entanglement allegedly induced by non-classical gravity and identify the experimental conditions required to perform successfully the BM [10, 11] and Krisnanda *et al* [12] proposals. Moreover, we also quantify the effective decoherence due to the action of the continuous spontaneous localization (CSL) model [53, 54], which is the most studied among the models of spontaneous wavefunction collapse.

2. Witnessing non-classical features of gravity

The proposals in references [10, 11] and that in reference [12] to test non-classical features of gravity are based on the generation of gravitationally induced entanglement. Indeed, a classical mediator cannot induce entanglement between two systems that are not directly interacting [55]. Therefore, the observation of gravitationally induced entanglement between two massive systems implies that the gravitational mediator displays non-classical features. We briefly review the two proposals.

2.1. BM proposal
The first setup proposed to test gravitationally-induced entanglement is that of Bose *et al* [10] and Marletto–Vedral [11] (BM). The setup is based on Stern–Gerlach interferometry [56–58], however alternative experimental schemes, as for example that exploiting magnetic levitation [59], can be also considered. Two diamond particles of mass m and radius R embedded with a single spin $1/2$ are initially prepared in the superposition state $(|\uparrow\rangle + |\downarrow\rangle)/\sqrt{2}$ and sent simultaneously through two Stern–Gerlach interferometers as depicted in figure 1(a). After passing through an inhomogeneous magnetic field, the spin superposition induces a position superposition for each of the particles, thus entangling the spin and the position. The composite state of the system thus becomes

$$|\psi\rangle_1 \otimes |\psi\rangle_2 \quad \text{where} \quad |\psi\rangle_i = \frac{|\uparrow, L\rangle_i + |\downarrow, R\rangle_i}{\sqrt{2}} \tag{1}$$

is the single particle state, and $|L\rangle$ and $|R\rangle$ are the localized states of the particles in the left and right branch of the interferometer, respectively. This assumption about the states of the particles has been shown to be a valid approximation for this setup [25].

Now gravity comes in play, mediating the interaction between the two masses. If gravity is to obey the quantum superposition principle, it induces a different phase for each of the parts of the superposition, which depends on the distance from the other branches of the superposition [10]. This interaction leads to an entangled state of the two masses [10, 11].

An estimate of the gravity-induced phases can be obtained by assuming that the dominant effect can be computed via Newtonian interaction [10, 11, 13, 18]; this approximation is valid also in the linearised quantum gravity model [1, 60]. In particular, with reference to the setup represented in figure 1(a), we assume that the gravitational interaction is sufficiently weak to not modify the relative distances between the branches but at the same time strong enough to modify the corresponding relative phases. Moreover, we assume that all other interactions among the two particles are negligible and we account for the action of gravity only in the parallel branches of the interferometers. In such a way, the problem is significantly simplified. The corresponding driving Hamiltonian, in the $\{|i\rangle_1 \otimes |j\rangle_2\}$ with $i, j = L, R$ basis representation, reads

$$H_{\mathrm{BM-g}} = \begin{pmatrix} U_0 & 0 & 0 & 0 \\ 0 & U_- & 0 & 0 \\ 0 & 0 & U_+ & 0 \\ 0 & 0 & 0 & U_0 \end{pmatrix}, \tag{2}$$

where we defined

$$U_0 = G\frac{m^2}{d}, \qquad U_\pm = G\frac{m^2}{d \mp \Delta x}, \tag{3}$$

with d denoting the distance between the centre of mass of the two particles and Δx the superposition distance. By assuming that the initial state is that in equation (1), the corresponding density matrix at time t reads:

$$\rho = \frac{1}{4} \begin{pmatrix} 1 & e^{-i\Delta_{0-}t} & e^{-i\Delta_{0+}t} & 1 \\ e^{i\Delta_{0-}t} & 1 & e^{-i\Delta_{-+}t} & e^{i\Delta_{0-}t} \\ e^{i\Delta_{0+}t} & e^{i\Delta_{-+}t} & 1 & e^{i\Delta_{0+}t} \\ 1 & e^{-i\Delta_{0-}t} & e^{-i\Delta_{0+}t} & 1 \end{pmatrix}, \tag{4}$$

with

$$\Delta_{ij} = \frac{U_i - U_j}{\hbar} \quad \text{with} \quad i, j \in \{0, +, -\}. \tag{5}$$

The entanglement of the density matrix ρ is verified by applying the Peres–Horodecki criterion [61, 62]. In particular, we calculate the eigenvalues $\tilde{\lambda}_i$ of the partially transposed density matrix, which we explicitly derive in appendix A. They read:

$$\tilde{\lambda}_1^\pm = \frac{1}{2}\left(1 \pm \left|\cos\frac{t}{\tau_G}\right|\right), \qquad \tilde{\lambda}_2^\pm = \pm\frac{1}{2}\left|\sin\frac{t}{\tau_G}\right|, \tag{6}$$

where we defined the characteristic time

$$\tau_G = \frac{\hbar d\left[\left(\frac{d}{\Delta x}\right)^2 - 1\right]}{Gm^2}. \tag{7}$$

According to the Peres–Horodecki criterion, the system is in an entangled state if at least one among the eigenvalues $\tilde{\lambda}_i$ is negative. The condition is both necessary and sufficient for 2×2 dimensional systems as in our case. We notice that $\tilde{\lambda}_2^-$ is always negative $\forall t \neq k\pi\tau_G$ with $k \in \mathbb{Z}$. We quantify the corresponding entanglement by exploiting the logarithmic negativity $E = \log_2 \|\tilde{\rho}\|_1$, where $\|\cdot\|_1$ is the trace norm [55]. This gives

$$E_{\mathrm{BM-free}} = \log_2\left(1 + \left|\sin\frac{t}{\tau_G}\right|\right). \tag{8}$$

The entanglement of the system has a periodic dynamics and reaches its first maximum value at time $t_{\mathrm{MAX}} = \frac{\pi}{2}\tau_G$. By inserting the values of the parameters chosen by Bose *et al* [10], which are reported in table 1, we have $t_{\mathrm{MAX}} \simeq 25$ s. We remark that the value of d has been chosen by Bose *et al* such that the Casimir–Polder interactions between the two spheres are 10 times smaller than the gravitational interaction. In this way, it is easier to discriminate the contribution of gravity to entanglement from that of these short-range forces. A slightly different setup with mitigated Casimir–Polder interactions has been recently proposed in [51] and thoroughly analysed in [52]. This setup proposes to insert a conducting plate between the two spheres and provides an improvement of one/two orders of magnitude on the mass and

Table 1. Numerical value of the parameters proposed in the setups by Bose *et al* [10], Marletto–Vedral [11] and by Krisnanda *et al* [12]. The masses m are assumed to be spheres of radius R and are separated by a distance d. For the BM setup one has a superposition distance of Δx, while in that of Krisnanda *et al* the masses are initially confined in an harmonic trap of frequency ω_0

Proposal	m (kg)	R (m)	d (m)	Δx (m)	ω_0 (Hz)
Bose	10^{-14}	10^{-6}	4.5×10^{-4}	2.5×10^{-4}	/
Marletto	10^{-12}	/	10^{-6}	/	/
Krisnanda	10^{-7}	10^{-4}	3×10^{-4}	/	10^5

superposition size with respect to [10]. The corresponding analysis of decoherence acting on the experimental apparatus and that due to external acceleration noises were performed in [63, 64] respectively, while the decoherence effects on the system were not quantified. In an attempt to simplify the treatment of the decoherence effects, here we will not consider this modified version of the setup, although our analysis can be applied also to this scenario.

2.2. Krisnanda *et al* proposal

The second setup we consider was recently proposed by Krisnanda *et al* in [12]. The setup is schematically depicted in figure 1(b) and consists of two osmium spheres of mass m and radius R that are initially trapped in harmonic potentials with frequency ω_0 separated by a distance d. The masses are assumed to be cooled down close to the ground state of their harmonic potentials, which is achievable with current technology [65, 66]. The particles are subsequently released from the traps and are let free to interact gravitationally and entangle. Again, the Newtonian potential can be exploited to effectively describe such an interaction. The quantification of the degree of entanglement can be provided through well established continuous variables techniques applied to bipartite Gaussian states [67]. In particular, in such a case, the separability of the state can be simply verified through its 4×4 covariance matrix in position and momentum.

In the proposal of Krisnanda *et al*, one assumes that the two masses are initially prepared in Gaussian thermal states of the harmonic potentials. Moreover, one can approximate the Newtonian potential to second order in the quantum fluctuations $(\hat{x}_A - \hat{x}_B)$ of the relative distance d [12]:

$$\hat{H}_{K-g} = -\frac{Gm^2}{d}\left(1 + \frac{(\hat{x}_A - \hat{x}_B)}{d} + \frac{(\hat{x}_A - \hat{x}_B)^2}{d^2}\right), \tag{9}$$

where the last term entangles the two masses [12, 68]. Under this approximation, which is valid for $|\hat{x}_A - \hat{x}_B| \ll d$ according to the parameters reported in table 1 and for a duration of the experiment of around 1 s [12], the dynamics is Gaussian. Krisnanda *et al* derived the analytic expression for the logarithmic negativity of the system in the limit $2Gm \ll \omega_0^2 d^3$ and $\sqrt{2Gm}\omega t \ll \omega_0 d^{3/2}$, which reads [12]:

$$E_{K-free} = -\log_2\left(\sqrt{1 + 2\sigma(t) - 2\sqrt{\sigma(t)^2 + \sigma(t)}}\right), \tag{10}$$

where $\sigma(t) = 4G^2 m^2 \omega_0^2 t^6 / 9d^6$. Using the parameters reported in table 1, after 1 s, the logarithmic negativity is 10^{-2}, a value which can be detected with current technology [69].

3. Decoherence effects

To measure the entanglement created by the quantum gravitational interaction one must ensure that environmental decoherence is sufficiently weak to not spoil such an effect. The main sources of decoherence are the scattering of residual gas and the scattering, emission and absorption of thermal photons. Here, we compute explicitly these effects on the dynamics of the system in the two setups above described, and their influence on the gravitationally-induced entanglement.

3.1. BM proposal

The effect of decoherence on the BM setup can be conveniently described in terms of a master equation, which in the position representation reads [70, 71]:

$$\frac{d\rho\left(\boldsymbol{x}, \boldsymbol{x}', t\right)}{dt} = -\frac{i}{\hbar}\left\langle \boldsymbol{x}\left|\left[\hat{H}, \hat{\rho}(t)\right]\right|\boldsymbol{x}'\right\rangle - \Gamma(|\boldsymbol{x} - \boldsymbol{x}'|)\rho(\boldsymbol{x}, \boldsymbol{x}', t), \tag{11}$$

Table 2. Values of a and Γ_0 entering in equation (12) which quantify the decoherence effects induced by collisions with air molecules (Air) and scattering (Sc), absorption (Ab) and emission (Em) of thermal photons on a sphere of radius R, dielectric constant ϵ and bulk temperature T_i [70, 71]. Here, m_{air} denotes the mass of the molecules of the residual air, T and P are respectively the temperature and the pressure at which the experiment is performed, and $\zeta(n)$ is the Riemann zeta function. To quantify the effects, one has $\epsilon = 5.7 + i \times 10^{-4}$ [72] for diamond used in the BM proposal, while $\epsilon = 0.6 + i \times 2.5$ [73] for osmium used in the Krisnanda proposal. Moreover, for the sake of simplicity, we take $T_i = T$ and $m_{air} \sim 6.6 \times 10^{-27}$ kg corresponding to a atom of helium.
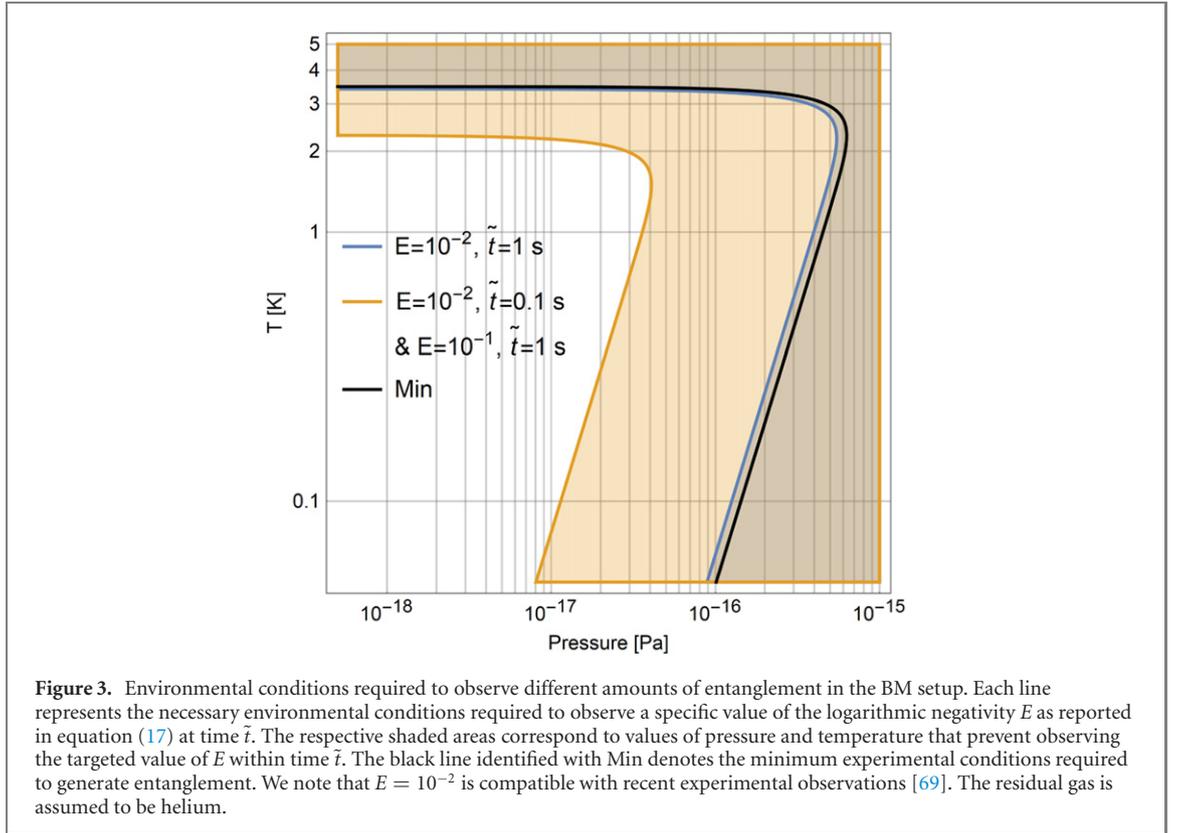
Source	a^i	Γ_0^i
Air	$\dfrac{\pi \hbar}{\sqrt{2\pi m_{air} k_B T}}$	$\dfrac{16\pi\sqrt{2\pi}}{3} \dfrac{PR^2}{\sqrt{m_{air} k_B T}}$
Sc	$\dfrac{\pi^{2/3}\hbar c}{2k_B T}$	$8! \dfrac{8\pi^{1/3}}{9} R^6 c \left(\dfrac{k_B T}{\hbar c}\right)^7 \zeta(9) \mathrm{Re}\left[\dfrac{\epsilon-1}{\epsilon+2}\right]^2$
Ab	$\dfrac{\pi^{2/3}\hbar c}{2k_B T}$	$\dfrac{16\pi^{19/3}}{189} R^3 c \left(\dfrac{k_B T}{\hbar c}\right)^4 \mathrm{Im}\dfrac{\epsilon-1}{\epsilon+2}$
Em	$\dfrac{\pi^{2/3}\hbar c}{2k_B T_i}$	$\dfrac{16\pi^{19/3}}{189} R^3 c \left(\dfrac{k_B T_i}{\hbar c}\right)^4 \mathrm{Im}\dfrac{\epsilon-1}{\epsilon+2}$

Figure 2. Entanglement indicators for the BM proposal. (Top panel) The eigenvalue $\tilde{\lambda}_2^-$ provided by equation (14) as function of time and of the localization strength Γ. The region $\tilde{\lambda}_2^- < 0$, which is below the black curve, corresponds to entangled states of the system. (Bottom panel) evolution of the logarithmic negativity of the system E given in equation (17) for different values of Γ.
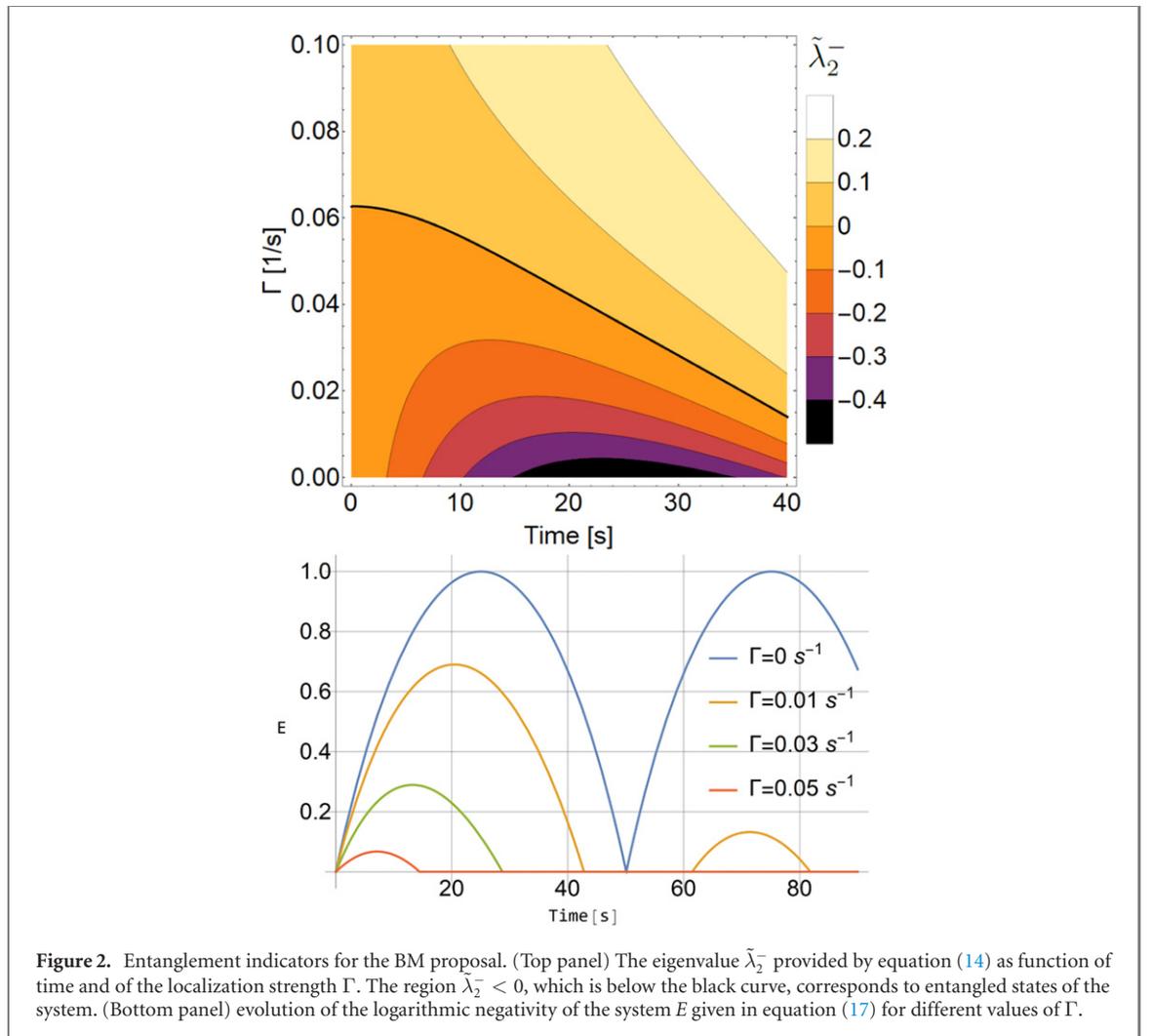
where $\hat{H}$ is the free Hamiltonian, $\rho(\boldsymbol{x}, \boldsymbol{x}', t) = \langle \boldsymbol{x} | \hat{\rho}(t) | \boldsymbol{x}' \rangle$ and we consider the common ansatz [71]

$$\Gamma(\Delta x) = \Gamma_0 \left(1 - \exp\left[-\frac{\Delta x^2}{4a^2}\right]\right). \tag{12}$$

Such a master equation leads to an exponential suppression in time of the off-diagonal terms of the density matrix in the position representation. According to equation (12), decoherence is characterized by the localization strength Γ_0 and localization distance a, whose explicit forms are reported in table 2. In the proposals under consideration, there are only four possible position configurations, thus the problem is

Figure 3. Environmental conditions required to observe different amounts of entanglement in the BM setup. Each line represents the necessary environmental conditions required to observe a specific value of the logarithmic negativity E as reported in equation (17) at time $\tilde{t}$. The respective shaded areas correspond to values of pressure and temperature that prevent observing the targeted value of E within time $\tilde{t}$. The black line identified with Min denotes the minimum experimental conditions required to generate entanglement. We note that $E = 10^{-2}$ is compatible with recent experimental observations [69]. The residual gas is assumed to be helium.

strongly simplified to a discrete description. Moreover, we assume that the decoherence acts independently on the two masses.

By starting from the common initial state defined in equation (1), the density matrix ρ of the system at time t reads:

$$\rho = \frac{1}{4} \begin{pmatrix} 1 & e^{-i\Delta_0 - t - \Gamma t} & e^{-i\Delta_0 + t - \Gamma t} & e^{-2\Gamma t} \\ e^{i\Delta_0 - t - \Gamma t} & 1 & e^{-i\Delta_- + t - 2\Gamma t} & e^{i\Delta_0 - t - \Gamma t} \\ e^{i\Delta_0 + t - \Gamma t} & e^{i\Delta_- + t - 2\Gamma t} & 1 & e^{i\Delta_0 + t - \Gamma t} \\ e^{-2\Gamma t} & e^{-i\Delta_0 - t - \Gamma t} & e^{-i\Delta_0 + t - \Gamma t} & 1 \end{pmatrix}, \tag{13}$$

where $\Gamma = \Gamma^{\mathrm{air}}(\Delta x) + \Gamma^{\mathrm{ph,\ sc}}(\Delta x) + \Gamma^{\mathrm{ph,abs}}(\Delta x) + \Gamma^{\mathrm{ph,em}}(\Delta x)$ is the sum of the effects due to the collisions of the residual air molecules and the scattering and absorption and emission of thermal photons. The entanglement is then quantified as in the free case via the Peres-Horodecki criterion [61, 62]. While the entire derivation is reported in appendix A, here we show the obtained eigenvalues $\tilde{\lambda}_i$ of the partially transposed density matrix:

$$\tilde{\lambda}_1^\pm = \frac{e^{-\Gamma t}}{2} \left(\cosh \Gamma t \pm \left| \cos \frac{t}{\tau_G} \right| \right),$$

$$\tilde{\lambda}_2^\pm = \frac{e^{-\Gamma t}}{2} \left(\sinh \Gamma t \pm \left| \sin \frac{t}{\tau_G} \right| \right), \tag{14}$$

where τ_G is defined in equation (7). We remind that entanglement can be achieved only for negative values of one of the above eigenvalues. Since $\cosh \Gamma t \geqslant 1$ and $\sinh \Gamma t \geqslant 0$, negative values can be achieved only by $\tilde{\lambda}_2^-$. This happens when

$$\Gamma < \frac{1}{\tau_G} = \frac{Gm^2}{\hbar d \left(\left(\frac{d}{\Delta x} \right)^2 - 1 \right)}, \tag{15}$$

or, equivalently, when

$$\tau_C > \tau_G, \tag{16}$$

where $\tau_C = 1/\Gamma$ is the coherence time of the system [70]. The corresponding logarithmic negativity reads:

$$E_{\mathrm{BM-dec}} = \max \left\{ 0, \log_2 \left[e^{-\Gamma t} \left(\cosh \Gamma t + \left| \sin \frac{t}{\tau_G} \right| \right) \right] \right\}. \tag{17}$$

In the upper panel of figure 2, we report $\tilde{\lambda}_2^-$ for different values of time and of Γ. In the bottom panel, we report the logarithmic negativity of the system for different values of Γ. In figure 3, we have plotted the environmental conditions of temperature and pressure required to reach different amounts of entanglement with the parameters of table 1. Given these parameters, we observe in figure 2 that for Γ greater than $1/\tau_G \simeq 0.06 \text{ s}^{-1}$ the system is separable at all times. This corresponds to pressures and temperatures highlighted by the blue line named 'Min' in figure 3. Moreover, we notice that one needs temperatures lower than 4 K and residual air pressures lower than 10^{-16} Pa to detect entanglement in the setup. With these pressures and temperatures, considerable amounts of entanglement are reached in about 1 s.

3.2. Krisnanda *et al* proposal

In the setup of Krisnanda *et al*, the effect of environmental decoherence on the system can be described by the Heisenberg–Langevin equations for the position $\hat{x}_j$ and momentum $\hat{p}_j$ operators of the two masses. In one dimension, these equations read [74]:

$$
\begin{aligned}
\frac{d\hat{x}_j(t)}{dt} &= \frac{i}{\hbar} \left[\hat{H}, \hat{x}_j(t) \right], \\
\frac{d\hat{p}_j(t)}{dt} &= \frac{i}{\hbar} \left[\hat{H}, \hat{p}_j(t) \right] - \gamma_\varepsilon \hat{p}_j(t) + \hat{\xi}_j(t).
\end{aligned}
\tag{18}
$$

where $\hat{H}$ is the free Hamiltonian of the system, γ_ε quantifies the dissipation of the environment and it is related to Γ_0 through [75]

$$
\gamma_\varepsilon = \frac{\Lambda \hbar^2}{m k_B \mathsf{T}},
\tag{19}
$$

with $\Lambda = \Gamma_0/4a^2$, m denoting the mass of the particle and T the temperature of the environment. $\hat{\xi}_j(t)$ is an environmental noise operator, which can be described in terms of its mean $\langle \hat{\xi}_j(t) \rangle_\varepsilon = 0$, where $\langle \cdot \rangle_\varepsilon$ denotes the average over the environmental degrees of freedom, and the two-time correlation function. In particular, the latter can be strongly simplified in the Markovian regime which can be achieved in the limit of high temperatures of the environment: $k_B \mathsf{T} \gg \hbar \omega$. In such a case, it reads [74, 75]:

$$
\frac{\langle \hat{\xi}_j(t)\hat{\xi}_j(t') + \hat{\xi}_j(t')\hat{\xi}_j(t) \rangle_\varepsilon}{2} = 2\hbar^2 \Lambda \delta(t - t'),
\tag{20}
$$

where $\delta(\cdot)$ is the Dirac delta. Using the parameters considered by Krisnanda *et al*, which are reported in table 1, we see that the high-temperature limit holds for $\mathsf{T} \gg 10^{-6}$ K.

We now apply equation (18) to the setup under consideration. By denoting with ω_0 the frequency of the harmonic potentials where the two particles are initially trapped, the Langevin equations for the adimensional quadratures $\hat{X}_j = \sqrt{m\omega_0/\hbar}\,\hat{x}_j$ and $\hat{P}_j = \hat{p}_j/\sqrt{(\hbar m \omega_0)}$, read

$$
\begin{aligned}
\frac{d\hat{X}_j}{dt} &= \omega_0 \hat{P}_j \quad \text{with} \quad j = A, B, \\
\frac{d\hat{P}_A}{dt} &= \omega_0 \eta \left(\hat{X}_A - \hat{X}_B \right) - \gamma_\varepsilon \hat{P}_A + \hat{\xi}'_A + k, \\
\frac{d\hat{P}_B}{dt} &= \omega_0 \eta \left(\hat{X}_B - \hat{X}_A \right) - \gamma_\varepsilon \hat{P}_B + \hat{\xi}'_B - k,
\end{aligned}
\tag{21}
$$

where we defined $\gamma_\varepsilon = \gamma^{\text{air}} + \gamma^{\text{ph, sc}} + \gamma^{\text{ph,abs}} + \gamma^{\text{ph,em}}$ and $\hat{\xi}'_j = \left(\hat{\xi}^{\text{air}}_j + \hat{\xi}^{\text{ph,sc}}_j + \hat{\xi}^{\text{ph,abs}}_j + \hat{\xi}^{\text{ph,em}}_j \right) / \sqrt{\hbar m \omega_0}$, and introduced the parameters
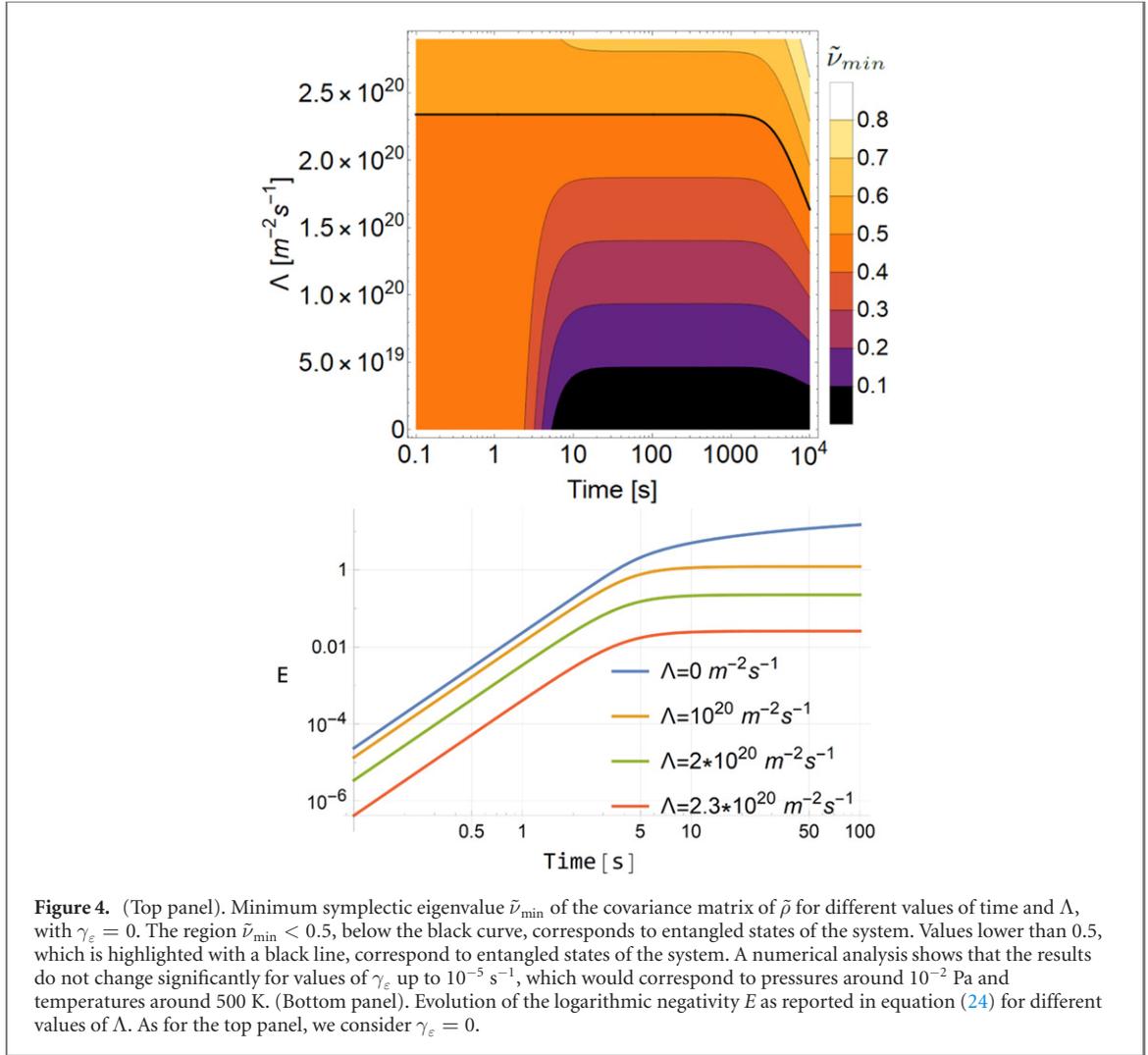
$$
\eta = \frac{2Gm}{\omega_0^2 d^3}, \quad \text{and} \quad k = \frac{Gm^2}{\sqrt{\hbar m \omega_0 d^4}}
\tag{22}
$$

which characterize the strength of the gravitational attraction [12]. We notice that, since the separation between the two spheres is much greater than the localization distances of the various processes, the noises acting on the two spheres can be safely considered as independent. Therefore, the two-time correlation function becomes

$$
\frac{\langle \hat{\xi}'_i(t)\hat{\xi}'_j(t') + \hat{\xi}'_j(t')\hat{\xi}'_i(t) \rangle}{2} = \frac{2\hbar\Lambda}{m\omega_0}\delta(t - t')\delta_{ij},
\tag{23}
$$

where $\Lambda = \Lambda^{\text{air}} + \Lambda^{\text{ph, sc}} + \Lambda^{\text{ph,abs}} + \Lambda^{\text{ph,em}}$.

The procedure that we use to calculate the logarithmic negativity of the system in this setup is reported thoroughly in appendix B and is here briefly outlined. First of all, we use the Langevin equation (21) to

Figure 4. (Top panel). Minimum symplectic eigenvalue $\tilde{\nu}_{\min}$ of the covariance matrix of $\tilde{\rho}$ for different values of time and Λ, with $\gamma_\varepsilon = 0$. The region $\tilde{\nu}_{\min} < 0.5$, below the black curve, corresponds to entangled states of the system. Values lower than 0.5, which is highlighted with a black line, correspond to entangled states of the system. A numerical analysis shows that the results do not change significantly for values of γ_ε up to 10^{-5} s^{-1}, which would correspond to pressures around 10^{-2} Pa and temperatures around 500 K. (Bottom panel). Evolution of the logarithmic negativity E as reported in equation (24) for different values of Λ. As for the top panel, we consider $\gamma_\varepsilon = 0$.

compute the covariance matrix $\boldsymbol{\sigma}$ for the quadratures $\hat{X}_j$ and $\hat{P}_j$. Using this matrix we can easily find the covariance matrix $\tilde{\boldsymbol{\sigma}}$ of the partially transposed state of the system $\tilde{\rho}$. The entanglement of the system can be calculated by using the so-called symplectic eigenvalues $\tilde{\nu}_i$ of $\tilde{\boldsymbol{\sigma}}$. For bipartite Gaussian states, the minimum $\tilde{\nu}_{\min}$ of these eigenvalues is smaller than $1/2$ if and only if the system is in an entangled state. Finally, the logarithmic negativity of the system can be expressed as [67]

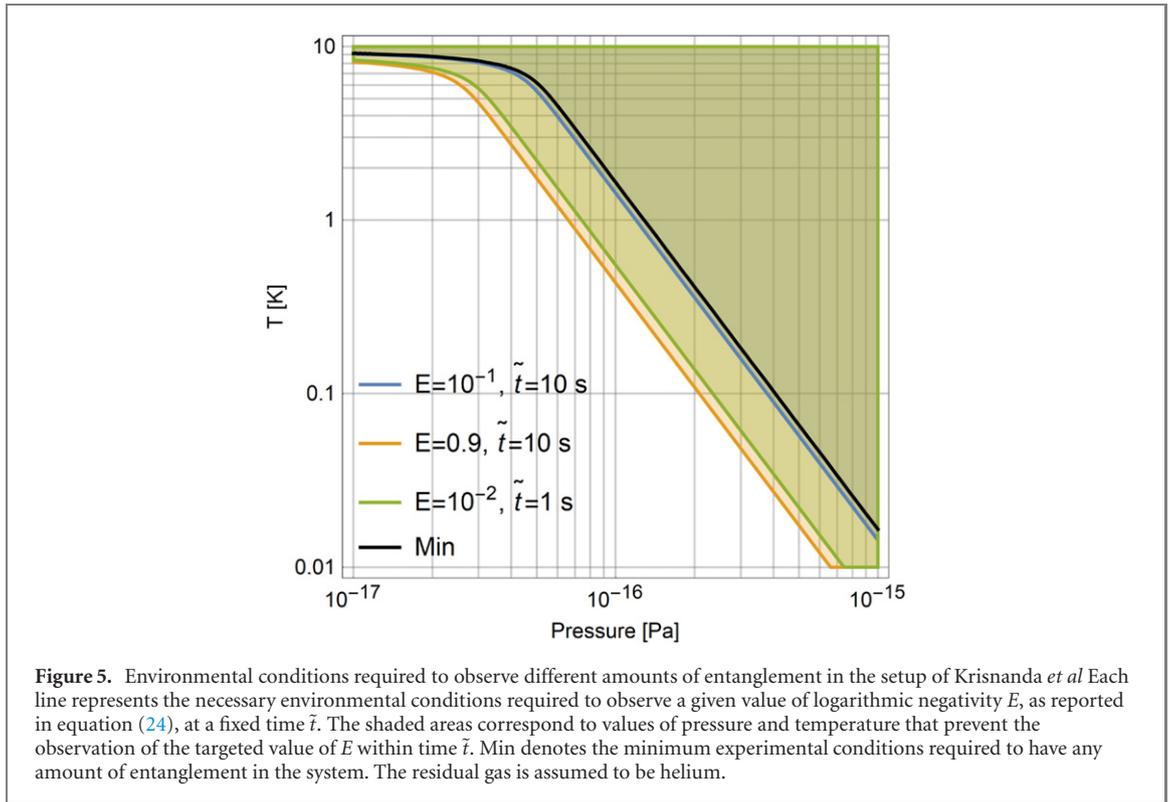$$E_{\text{K}-\text{dec}} = -\log_2(2\tilde{\nu}_{\min}). \tag{24}$$

The explicit expression for $\tilde{\nu}_{min}$ is cumbersome and we report it in appendix B. Here, we report its behaviour for small times:

$$\tilde{\nu}_{\min} = \frac{1}{2} + \frac{1}{2}\left(\frac{2\hbar\Lambda}{m\omega_0} - \eta\omega_0 - \gamma_\varepsilon\right)t + \mathcal{O}(t^2). \tag{25}$$

Comparing the term $2\hbar\Lambda/m\omega_0$ with the value of γ_ε given in equation (19), we notice that $\gamma_\varepsilon \ll 2\hbar\Lambda/m\omega_0$ when $\mathsf{T} \gg \hbar\omega/k_{\text{B}} \approx 10^{-6}$ K. If we work in this limit, we can safely neglect γ_ε in equation (25) and we have that $\tilde{\nu}_{\min} < 1/2$, thus indicating that the system is in an entangled state, when $2\hbar\Lambda/m\omega_0 < \eta\omega_0$. Notably, this latter condition can be rewritten as

$$\Lambda < \frac{Gm^2}{\hbar d^3}, \tag{26}$$

which coincides with the condition in equation (15) in the limit of $\Delta x \ll d$ once one considers the short-wavelength approximation in equation (12), i.e. $\Gamma \simeq \Lambda\Delta x^2$ which is valid for $\Delta x \ll a$. Thus, both equations (15) and (26) can be synthesised as equation (16): to generate gravitational induced entanglement, the characteristic time of entanglement creation must be shorter than the decoherence time characterizing the interaction of the system with its surrounding environment.

Figure 5. Environmental conditions required to observe different amounts of entanglement in the setup of Krisnanda *et al* Each line represents the necessary environmental conditions required to observe a given value of logarithmic negativity *E*, as reported in equation (24), at a fixed time $\tilde{t}$. The shaded areas correspond to values of pressure and temperature that prevent the observation of the targeted value of *E* within time $\tilde{t}$. Min denotes the minimum experimental conditions required to have any amount of entanglement in the system. The residual gas is assumed to be helium.

For later times, the behaviour of the entanglement can be seen in the upper panel of figure 4 where we report $\tilde{\nu}_{\min}$ for different values of time and of Λ, with $\gamma_\varepsilon = 0$. A numerical analysis shows that the results do not change appreciably for values of γ_ε up to 10^{-5} s^{-1}, which correspond to pressures around 10^{-2} Pa and temperatures around 500 K. In the bottom panel of figure 4 we show the time evolution of the logarithmic negativity $E_{\text{K}-\text{dec}}$ of the system for different values of Λ. Finally, in figure 5 we show the environmental conditions required to obtain a specific amount of entanglement at fixed times with the parameters of table 1. We notice that one needs temperatures lower than 9 K and residual air pressures around 10^{-16} Pa to have entanglement. With these pressures and temperatures, considerable amounts of entanglement are reached in about 10 s.

4. CSL model

In addition to environmental decoherence, we study also the possible effects of the CSL model on the two setups. This is the most studied among collapse models [32, 33]. The CSL model proposes a non-linear and stochastic modification of the Schrödinger equation. This modification induces the collapse of the wavefunction for macroscopic systems while it leaves the dynamics of microscopic systems almost unaffected [32, 33]. The collapse of the wavefunction causes the suppression of quantum superpositions and thus of any non-classical correlation, such as entanglement. CSL is quantified in terms of two parameters λ and r_C, which describe respectively the frequency of the collapse and its spatial resolution. Theoretical proposals include [53, 54, 76, 77]:

$$r_C = 10^{-7} \text{ m}, \quad \text{and} \quad \lambda = (10^{-17} \div 10^{-9}) \text{ s}^{-1}. \tag{27}$$

Larger values of λ are experimentally excluded. For further details we refer to [36] and references therein. We now apply CSL to the two setups we are considering.

4.1. BM proposal
Since, in the BM proposal, the distance d between the two masses is greater than r_C [cf table 1], one can safely neglect possible correlations of the noise and describe the CSL effect by simply using equation (11). According to CSL, $a = r_C$, while Γ_0 depends on the geometry of the system. In particular, for a

homogeneous sphere of mass m and radius R, Γ_0 reads [78]:

$$\Gamma_0^{\text{CSL}} = \lambda \frac{6m^2 r_{\text{C}}^4}{m_0^2 R^4} \left[1 - \frac{2r_{\text{C}}^2}{R^2} + e^{-\frac{R^2}{r_{\text{C}}^2}} \left(1 + \frac{2r_{\text{C}}^2}{R^2} \right) \right]. \tag{28}$$

Consequently, by exploiting the relation in equation (15), one finds that gravitationally induced entanglement can be generated only for $\lambda \lesssim 10^{-24}$ s^{-1} at $r_{\text{C}} = 10^{-7}$ m. This value is seven orders of magnitude smaller than the theoretical estimates on the lower bound on λ. Therefore we conclude that any value of the CSL parameters proposed in the literature would prevent the creation of entanglement in the BM setup.

4.2. Krisnanda *et al* proposal

For the setup of Krisnanda *et al*, we quantify the effect of the CSL model using the Langevin equation (18), where we substitute the second equation with [78, 79]:

$$\frac{d\hat{p}_j(t)}{dt} = \frac{i}{\hbar} \left[\hat{p}_j(t), \hat{H} \right] + \xi^{\text{CSL}}(t), \tag{29}$$

where $\xi^{\text{CSL}}(t)$ is a real-valued white noise with zero mean and correlation function reading [80]

$$\langle \xi_i^{\text{CSL}}(t) \xi_j^{\text{CSL}}(t') \rangle = 2\Lambda^{\text{CSL}} \hbar^2 \delta(t - t') \delta_{ij}, \tag{30}$$

with $\langle \cdot \rangle$ denoting the average over the realizations of the noise, and $\Lambda^{\text{CSL}} = \Gamma_0^{\text{CSL}}/4r_{\text{C}}^2$. Since the distance between the two spheres is much larger than r_{C}, the CSL noise acts independently on the two masses. Accordingly to CSL, there is no dissipation. Therefore, equation (26), where Λ is substituted by Λ^{CSL}, holds true for small times and defines the regime where gravitationally induced entanglement can be generated. By using the values of the parameters in table 1, the latter condition is satisfied for $\lambda \lesssim 10^{-23}$ s^{-1} at $r_{\text{C}} = 10^{-7}$ m, which is six orders of magnitude smaller than the lower value in equation (27). Therefore, the same conclusion as for the BM proposal holds: the presence of the CSL noise would prevent the creation of entanglement in the setup.

5. Conclusions

In this paper, we have studied decoherence effects on the gravitationally induced entanglement in the setups of BM [10, 11] and Krisnanda *et al* [12]. We have found an analytic expression for the entanglement when decoherence is explicitly considered in the dynamics of the system. Moreover, we have determined the maximum strength of decoherence, quantified by the expression in equation (16), which allows for gravitationally-induced entanglement generation in these setups. Such an expression also provides the ground to set the requirements of temperature and pressure necessary to perform the experiment.

The numerical analysis has shown that temperatures and pressures as low as 1 K and 10^{-16} Pa are sufficient for generating entanglement with $E = 10^{-2}$ after 0.15 s for the BM proposal and after 1.1 s for the Krisnanda proposal. Notably, cryogenic experiments can easily provide temperatures reaching 10 mK and pressures down to 10^{-16} Pa have already been reached in experiments with Penning traps [81]. However, the time-scale involved requires a free-falling particle to fall for 10 cm and 6.2 m respectively for the BM and the Krisnanda proposals. Clearly, maintaining the above conditions of temperature and pressure can be technically challenging. As pointed out in [10], milder environmental conditions such as $P = 10^{-15}$ Pa would lead to a decoherence time of the order of a few seconds, which is comparable to the time of the experiment. However, such conditions would invalidate the BM proposal, while the Krisnanda proposal would work only for lower temperatures $\leqslant 10$ mK. Moreover the two particles should remain aligned during the experiments, one should also prepare the system without any horizontal and vertical relative velocity, which, over time, would change the relative distance thus potentially disrupting the experiments. Table 3 compares the free-fall times and corresponding heights necessary for the two proposals at different environmental conditions. While entanglement could be difficult to generate, one could rely on other non-classical correlations such as discord [6], but this was beyond the aim of the current work.

In addition to environmental decoherence, we have also considered the effect of the CSL model on the two setups. We have shown that any proposed value of the CSL parameters would prevent the creation of entanglement in the two setups. We note that this was previously noted by Bose *et al* [10] for the BM proposal. Conversely, if gravitationally induced entanglement were observed in such setups, it would rule out the CSL model by $6 \sim 7$ orders of magnitude. Such an achievement would improve the current bounds [36] by more than 13 orders of magnitude, showcasing the necessity of a strong improvement of the

Table 3. Free-fall times t and heights $h = \frac{1}{2}gt^2$, with $g \simeq 9.8$ m s^{-2}, required to generate the amount E of entanglement at fixed values of temperature T and pressure P for the proposals of BM and Krisnanda.

Proposal	T (K)	P (Pa)	E	T (s)	H (m)
BM	1	10^{-16}	10^{-2}	0.15	0.1
	1	10^{-16}	10^{-1}	1.5	11
	1	10^{-15}	No generation	/	/
	10^{-2}	10^{-15}	No generation	/	/
Krisnanda	1	10^{-16}	10^{-2}	1.1	6.2
	1	10^{-16}	10^{-1}	2.9	42
	1	10^{-15}	No generation	/	/
	10^{-2}	10^{-15}	10^{-2}	1.2	7.6

state-of-art technology to successfully perform these experiments. On the contrary, one expects no effects from a stochastic gravitational wave background [82].

Finally, given the generality of the approaches used to consider explicitly the decoherence effects in the dynamics of the system, the results that we have obtained can be easily generalized to similar setups [27, 28] or to different decohering mechanisms, such as gravitational decoherence [83].

Acknowledgments

Data availability statement

No new data were created or analysed in this study.

Appendix A. Entanglement for the BM proposal

Here, we derive the eigenvalues of the partially transposed density matrix in the case of the BM proposal. The analysis is performed in the case of absence and presence of decoherence effects.

A.1. Case with no decoherence

If we assume that the initial state of the system is $(|\uparrow\rangle_1 + |\downarrow\rangle_1) \otimes (|\uparrow\rangle_2 + |\downarrow\rangle_2)/2$, the initial density matrix in the $\{|i\rangle_1 \otimes |j\rangle_2, i,j = \uparrow, \downarrow\}$ basis reads:

$$\rho(0) = \frac{1}{4} \begin{pmatrix} 1 & 1 & 1 & 1 \\ 1 & 1 & 1 & 1 \\ 1 & 1 & 1 & 1 \\ 1 & 1 & 1 & 1 \end{pmatrix}. \tag{A1}$$

The density matrix at time t is given by $\rho(t) = e^{-iHt/\hbar}\rho(0)e^{iHt/\hbar}\rho$ which, using the Hamiltonian of equation (2), reads:

$$\rho(t) = \frac{1}{4} \begin{pmatrix} 1 & e^{-i\Delta_{0-}t} & e^{-i\Delta_{0+}t} & 1 \\ e^{i\Delta_{0-}t} & 1 & e^{-i\Delta_{-+}t} & e^{i\Delta_{0-}t} \\ e^{i\Delta_{0+}t} & e^{i\Delta_{-+}t} & 1 & e^{i\Delta_{0+}t} \\ 1 & e^{-i\Delta_{0-}t} & e^{-i\Delta_{0+}t} & 1 \end{pmatrix}, \tag{A2}$$

Let us consider the partial transposition of ρ with respect to the second system:

$$\tilde{\rho}(t) = \frac{1}{4} \begin{pmatrix} 1 & e^{i\Delta_{0-}t} & e^{-i\Delta_{0+}t} & e^{-i\Delta_{-+}t} \\ e^{-i\Delta_{0-}t} & 1 & 1 & e^{i\Delta_{0-}t} \\ e^{i\Delta_{0+}t} & 1 & 1 & e^{-i\Delta_{0+}t} \\ e^{i\Delta_{-+}t} & e^{-i\Delta_{0-}t} & e^{i\Delta_{0+}t} & 1 \end{pmatrix}, \tag{A3}$$

The eigenvalues of $\tilde{\rho}$ can be easily evaluated and are those reported in equation (6).

A.2. Case with decoherence

When the system is subject to decoherence, the density matrix of the system at time t can be calculated using equation (11):

$$\rho(t) = \frac{1}{4} \begin{pmatrix} 1 & e^{-i\Delta_0-t-\Gamma t} & e^{-i\Delta_0+t-\Gamma t} & e^{-2\Gamma t} \\ e^{i\Delta_0-t-\Gamma t} & 1 & e^{-i\Delta_-+t-2\Gamma t} & e^{i\Delta_0-t-\Gamma t} \\ e^{i\Delta_0+t-\Gamma t} & e^{i\Delta_-+t-2\Gamma t} & 1 & e^{i\Delta_0+t-\Gamma t} \\ e^{-2\Gamma t} & e^{-i\Delta_0-t-\Gamma t} & e^{-i\Delta_0+t-\Gamma t} & 1 \end{pmatrix}. \tag{A4}$$

Again, if we consider the partial transposition of ρ with respect to the second system we get:

$$\tilde{\rho}(t) = \frac{1}{4} \begin{pmatrix} 1 & e^{i\Delta_0-t-\Gamma t} & e^{-i\Delta_0+t-\Gamma t} & e^{-i\Delta_-+t-2\Gamma t} \\ e^{-i\Delta_0-t-\Gamma t} & 1 & e^{-2\Gamma t} & e^{i\Delta_0-t-\Gamma t} \\ e^{i\Delta_0+t-\Gamma t} & e^{-2\Gamma t} & 1 & e^{-i\Delta_0+t-\Gamma t} \\ e^{i\Delta_-+t-2\Gamma t} & e^{-i\Delta_0-t-\Gamma t} & e^{i\Delta_0+t-\Gamma t} & 1 \end{pmatrix}, \tag{A5}$$

whose correspondent eigenvalues are given by equation (14).

Appendix B. Symplectic eigenvalues—Krisnanda *et al*

In order to calculate the logarithmic negativity of the system, we first find its covariance matrix. This can be done in the following way. First, if we define

$$\hat{u}(t) = \begin{pmatrix} \hat{X}_A(t) \\ \hat{P}_A(t) \\ \hat{X}_B(t) \\ \hat{P}_B(t) \end{pmatrix}, \tag{B1}$$

in terms of which we can rewrite equation (21) in a more compact way:

$$\frac{d\hat{u}(t)}{dt} = K\hat{u}(t) + \hat{\ell}(t) + \kappa, \tag{B2}$$

where we introduced

$$K = \begin{pmatrix} 0 & \omega & 0 & 0 \\ \omega\eta & -\gamma_\varepsilon & -\omega\eta & 0 \\ 0 & 0 & 0 & \omega \\ -\omega\eta & 0 & \omega\eta & -\gamma_\varepsilon \end{pmatrix}, \quad \hat{\ell}(t) = \begin{pmatrix} 0 \\ \hat{\xi}'_A \\ 0 \\ \hat{\xi}'_B \end{pmatrix}, \quad \kappa = \begin{pmatrix} 0 \\ k \\ 0 \\ -k \end{pmatrix}. \tag{B3}$$

The solution of equation (B2) reads:

$$\hat{u}(t) = W_+(t)\hat{u}(0) + W_+(t)\int_0^t dt' W_-(t')[\hat{\ell}(t') + \kappa], \tag{B4}$$

where $W_\pm = e^{\pm Kt}$. This expression can be used to calculate the covariance matrix of the system. Its elements are defined as:

$$\sigma_{ij}(t) = \frac{\langle \hat{u}_i(t)\hat{u}_j(t) + \hat{u}_j(t)\hat{u}_i(t) \rangle}{2} - \langle \hat{u}_i(t) \rangle \langle \hat{u}_j(t) \rangle, \tag{B5}$$

where $\langle \cdot \rangle$ denotes the average over the initial state and over the environmental degrees of freedom if the case with decoherence is considered. Using equation (B4), we can calculate $\sigma(t)$ as:

$$\sigma(t) = W_+(t)\sigma(0)W_+^T(t) + W_+(t)\left[\int_0^t dt' \, W_-(t')DW_-^T(t')\right] W_+^T(t), \tag{B6}$$

where $W_\pm^T$ denotes the transposed of $W_\pm$ and $D = \mathrm{diag}(0, \mu\omega_0, 0, \mu\omega_0)$, with $\mu = 2\hbar\Lambda/m\omega_0^2$. Now, if we divide $\sigma(t)$ in the following 2×2 submatrices:

$$\sigma = \begin{pmatrix} \alpha & \gamma \\ \gamma^T & \beta \end{pmatrix}, \tag{B7}$$

we can calculate the symplectic eigenvalues of the covariance matrix of the partially transposed state in the following way [67]:

$$\tilde{\nu}_{\mp} = \frac{\sqrt{\tilde{\Delta}(\boldsymbol{\sigma}) \mp \sqrt{\tilde{\Delta}(\boldsymbol{\sigma})^2 - 4 \operatorname{Det}\boldsymbol{\sigma}}}}{\sqrt{2}}, \tag{B8}$$

where we defined

$$\tilde{\Delta}(\boldsymbol{\sigma}) = \operatorname{Det}\boldsymbol{\alpha} + \operatorname{Det}\boldsymbol{\beta} - 2\operatorname{Det}\boldsymbol{\gamma}. \tag{B9}$$

The smallest of these symplectic eigenvalues is related to the logarithmic negativity of the system via $E = -\log_2(2\tilde{\nu}_{\min})$.

If we assume to start in the ground state of the two harmonic traps, the initial covariance matrix appearing in equation (B6) reads:

$$\boldsymbol{\sigma}(0) = \frac{1}{2} \begin{pmatrix} 1 & 0 & 0 & 0 \\ 0 & 1 & 0 & 0 \\ 0 & 0 & 1 & 0 \\ 0 & 0 & 0 & 1 \end{pmatrix}. \tag{B10}$$

We use $\boldsymbol{\sigma}(0)$ to find the solution of equation (B6) and the symplectic eigenvalues of the partially transposed covariance matrix via equation (B8). The general expression for $\tilde{\nu}_{\min}$ is cumbersome but expanding $\tilde{\nu}_{\min}$ around $\tau = 0$, where $\tau = \omega_0 t$, we get:

$$\tilde{\nu}_{\min}(\tau) = \frac{1}{2} + \frac{1}{2}\left(\mu - \eta - \frac{\gamma_\varepsilon}{\omega_0}\right)\tau + O(\tau^2). \tag{B11}$$

Replacing τ with $\omega_0 t$ in equation (B11) we get equation (25).

If we neglect γ_ε, as discussed in the section 3, the analytic expression for $\tilde{\nu}_{\min}$ becomes much simpler:

$$\tilde{\nu}_{\min}(\tau) = \frac{1}{8\sqrt{3}\eta}\sqrt{a(\tau) - \sqrt{a^2(\tau) - b(\tau)}}, \tag{B12}$$

where a and b are given by:

$$\begin{aligned} a(\tau) = {} & 2\eta\left[4\eta^2\left(2\mu\tau^3 + 3\tau^2 + 3\right) + 2\eta\left(2\mu\tau^3 + 3\tau^2 + 6\mu\tau + 6\right) - 6\mu^2\tau^2 + 3\right]\cosh\left(2\sqrt{2\eta}\tau\right) \\ & - 2\eta\left[4\eta^2\left(2\mu\tau^3 + 3\tau^2 + 3\right) - 2\eta\left(4\mu^2\tau^4 + 8\mu\tau^3 + 3\tau^2 + 12\mu\tau + 6\right) + 6\mu^2\tau^2 + 6\mu\tau + 3\right] \\ & - \sqrt{2\eta}\left[24\eta^2\tau(\mu\tau + 1) + \eta\left(-6\mu - 4\mu^2\tau^3 + 6\mu\tau^2 + 12\tau\right) - 3\mu(2\mu\tau + 1)\right]\sinh\left(2\sqrt{2\eta}\tau\right), \end{aligned} \tag{B13}$$

$$\begin{aligned} b(\tau) = {} & 96\eta^2\left(\mu^2\tau^4 + 2\mu\tau^3 + 6\mu\tau + 3\right)\left[8\mu\eta^2\tau + 8\eta^2 - \mu^2 - 4\mu^2\eta\tau^2 + \mu^2\cosh\left(2\sqrt{2\eta}\tau\right) - 4\mu\eta\tau \right. \\ & \left. + \sqrt{2\eta}(2\eta + 1)\mu\sinh\left(2\sqrt{2\eta}\tau\right)\right]. \end{aligned} \tag{B14}$$

This expression is easier to handle and has been used to plot $\tilde{\nu}_{\min}$ and E in figure 4.

ORCID iDs

Simone Rijavec ⬡ https://orcid.org/0000-0002-2210-6274
Matteo Carlesso ⬡ https://orcid.org/0000-0002-9929-7291
Angelo Bassi ⬡ https://orcid.org/0000-0001-7500-387X
Chiara Marletto ⬡ https://orcid.org/0000-0002-2690-4433

References

[1] Kiefer C 2007 *Quantum Gravity* 2nd edn (New York: Oxford University Press)
[2] Rothman T and Boughn S 2006 *Found. Phys.* **36** 1801
[3] Dyson F 2013 *Int. J. Mod. Phys.* A **28** 1330041
[4] Pikovski I, Vanner M R, Aspelmeyer M, Kim M S and Brukner Č 2012 *Nat. Phys.* **8** 393
[5] Carney D, Stamp P C E and Taylor J M 2019 *Class. Quantum Grav.* **36** 034001
[6] Carlesso M, Bassi A, Paternostro M and Ulbricht H 2019 *New J. Phys.* **21** 093052
[7] Al Balushi A, Cong W and Mann R B 2018 *Phys. Rev.* A **98** 043811
[8] Parikh M, Wilczek F and Zahariade G 2020 (arXiv:2010.08205[hep-th])
[9] Kafri D, Taylor J M and Milburn G J 2014 *New J. Phys.* **16** 065020

[10]   Bose S *et al* 2017 *Phys. Rev. Lett.* **119** 240401
[11]   Marletto C and Vedral V 2017 *Phys. Rev. Lett.* **119** 240402
[12]   Krisnanda T, Tham G Y, Paternostro M and Paterek T 2020 *npj Quantum Inf.* **6** 12
[13]   Belenchia A, Wald R M, Giacomini F, Castro-Ruiz E, Brukner C and Aspelmeyer M 2018 *Phys. Rev.* D **98** 126009
[14]   Altamirano N, Corona-Ugalde P, Mann R B and Zych M 2018 *Class. Quantum Grav.* **35** 145005
[15]   Khosla K E and Nimmrichter S 2018 (arXiv:1812.03118[quant-ph])
[16]   Hall M J W and Reginatto M 2018 *J. Phys. A: Math. Theor.* **51** 085303
[17]   Anastopoulos C and Hu B-L 2018 (arXiv:1804.11315[quant-ph])
[18]   Christodoulou M and Rovelli C 2019 *Phys. Lett.* B **792** 64
[19]   Belenchia A, Wald R M, Giacomini F, Castro-Ruiz E, Brukner Č and Aspelmeyer M 2019 *Int. J. Mod. Phys.* D **28** 1943001
[20]   Marletto C and Vedral V 2017 *npj Quantum Inf.* **3** 29
[21]   Marletto C and Vedral V 2020 *Phys. Rev.* D **102** 086012
[22]   Marshman R J, Mazumdar A and Bose S 2020 *Phys. Rev.* A **101** 052110
[23]   Marletto C and Vedral V 2017 *Nature* **547** 156
[24]   Bhole G, Jones J A, Marletto C and Vedral V 2020 *J. Phys. Commun.* **4** 025013
[25]   Chevalier H, Paige A J and Kim M S 2020 *Phys. Rev.* A **102** 022428
[26]   Miki D, Matsumura A and Yamamoto K 2021 *Phys. Rev.* D **103** 026017
[27]   Christodoulou M and Rovelli C 2020 *Front. Phys.* **8** 207
[28]   Christodoulou M, Biagio A D and Martin-Dussaud P 2020 (arXiv:2007.08431[gr-qc])
[29]   Miao H, Martynov D, Yang H and Datta A 2020 *Phys. Rev.* A **101** 063804
[30]   Howl R, Vedral V, Christodoulou M, Rovelli C, Naik D and Iyer A 2020 (arXiv:2004.01189[quant-ph])
[31]   Matsumura A and Yamamoto K 2020 *Phys. Rev.* D **102** 106021
[32]   Bassi A and Ghirardi G 2003 *Phys. Rep.* **379** 257
[33]   Bassi A, Lochan K, Satin S, Singh T P and Ulbricht H 2013 *Rev. Mod. Phys.* **85** 471
[34]   Adler S L, Bassi A, Carlesso M and Vinante A 2019 *Phys. Rev.* D **99** 103001
[35]   Zheng D *et al* 2020 *Phys. Rev. Research* **2** 013057
[36]   Vinante A, Carlesso M, Bassi A, Chiasera A, Varas S, Falferi P, Margesin B, Mezzena R and Ulbricht H 2020 *Phys. Rev. Lett.* **125** 100404
[37]   Vinante A, Gasbarri G, Timberlake C, Toroš M and Ulbricht H 2020 *Phys. Rev. Research* **2** 043229
[38]   Terashima H and Ueda M 2004 *Phys. Rev.* A **69** 032113
[39]   Terashima H and Ueda M 2005 *J. Phys. A: Math. Gen.* **38** 2029
[40]   Esfahani B N and Dehdashti S 2007 *Int. J. Theor. Phys.* **46** 1495
[41]   Ahmadi F and Mehrafarin M 2012 *J. Phys. A: Math. Theor.* **45** 485302
[42]   Ahmadi F and Mehrafarin M 2014 *Quantum Inf. Process.* **13** 639
[43]   Ralph T C and Pienaar J 2014 *New J. Phys.* **16** 085008
[44]   Gooding C and Unruh W G 2014 *Phys. Rev.* D **90** 044071
[45]   Pikovski I, Zych M, Costa F and Brukner Č 2015 *Nat. Phys.* **11** 668
[46]   Gooding C and Unruh W G 2015 *Found. Phys.* **45** 1166
[47]   Carlesso M and Bassi A 2016 *Phys. Lett.* A **380** 2354
[48]   Pang B H, Chen Y and Khalili F Y 2016 *Phys. Rev. Lett.* **117** 090401
[49]   Plato A D K, Hughes C N and Kim M S 2016 *Contemp. Phys.* **57** 477
[50]   Dehdashti S, Avazzadeh Z, Xu Z, Shen J Q, Mirza B and Wang H 2017 *Sci. Rep.* **7** 15046
[51]   Nguyen H C and Bernards F 2020 *Eur. Phys. J.* D **74** 69
[52]   van de Kamp T W, Marshman R J, Bose S and Mazumdar A 2020 *Phys. Rev.* A **102** 062807
[53]   Ghirardi G C, Pearle P and Rimini A 1990 *Phys. Rev.* A **42** 78
[54]   Ghirardi G C, Grassi R and Benatti F 1995 *Found. Phys.* **25** 5
[55]   Horodecki R, Horodecki P, Horodecki M and Horodecki K 2009 *Rev. Mod. Phys.* **81** 865
[56]   Machluf S, Japha Y and Folman R 2013 *Nat. Comm.* **4** 2424
[57]   Wan C, Scala M, Morley G W, Rahman A A, Ulbricht H, Bateman J, Barker P F, Bose S and Kim M S 2016 *Phys. Rev. Lett.* **117** 143003
[58]   Amit O *et al* 2019 *Phys. Rev. Lett.* **123** 083601
[59]   Pino H, Prat-Camps J, Sinha K, Venkatesh B P and Romero-Isart O 2018 *Quantum Sci. Technol.* **3** 025001
[60]   Marletto C and Vedral V 2018 *Phys. Rev.* D **98** 046001
[61]   Peres A 1996 *Phys. Rev. Lett.* **77** 1413
[62]   Horodecki P 1997 *Phys. Lett.* A **232** 333
[63]   Toroš M, van de Kamp T W, Marshman R J, Kim M S, Mazumdar A and Bose S 2020 (arXiv:2007.15029[gr-qc])
[64]   Großardt A 2020 *Phys. Rev.* A **102** 040202
[65]   Chan J, Alegre T P M, Safavi-Naeini A H, Hill J T, Krause A, Gröblacher S, Aspelmeyer M and Painter O 2011 *Nature* **478** 89
[66]   Teufel J D *et al* 2011 *Nature* **475** 359
[67]   Serafini A 2017 *Quantum Continuous Variables: A Primer of Theoretical Methods* (Boca Raton, FL: CRC Press)
[68]   Qvarfort S, Bose S and Serafini A 2020 *J. Phys. B: At. Mol. Opt. Phys.* **53** 235501
[69]   Palomaki T A, Teufel J D, Simmonds R W and Lehnert K W 2013 *Science* **342** 710
[70]   Schlosshauer M 2007 *Decoherence and the Quantum-To-Classical Transition* (Berlin: Springer)
[71]   Romero-Isart O 2011 *Phys. Rev.* A **84** 052121
[72]   Derkach V N, Golovashehenko R V, Nedukh S V, Plevako A S and Tarapov S I 2005 *2005 Joint 30th Int. Conf. on Infrared and Millimeter Waves and 13th Int. Conf. on Terahertz Electronics* vol 1 192−3
[73]   Windt D L, Cash W C, Scott M, Arendt P, Newnam B, Fisher R F and Swartzlander A B 1988 *Appl. Opt.* **27** 246
[74]   Giovannetti V and Vitali D 2001 *Phys. Rev.* A **63** 023812
[75]   Breuer H-P and Petruccione F 2002 *The Theory of Open Quantum Systems* (New York: Oxford University Press)
[76]   Ghirardi G C, Rimini A and Weber T 1986 *Phys. Rev.* D **34** 470
[77]   Adler S L 2007 *J. Phys. A: Math. Theor.* **40** 2935
[78]   Vinante A, Bahrami M, Bassi A, Usenko O, Wijts G and Oosterkamp T H 2016 *Phys. Rev. Lett.* **116** 090402
[79]   Bahrami M, Paternostro M, Bassi A and Ulbricht H 2014 *Phys. Rev. Lett.* **112** 210404

[80] Carlesso M, Bassi A, Falferi P and Vinante A 2016 *Phys. Rev.* D **94** 124036
[81] Sellner S *et al* 2017 *New J. Phys.* **19** 083023
[82] Toroš M, Mazumdar A and Bose S 2020 (arXiv:2008.08609[gr-qc])
[83] Bassi A, Großardt A and Ulbricht H 2017 *Class. Quantum Grav.* **34** 193002